New tools for rapid clinical and bioagent diagnostics: microwaves and plasmonic nanostructures

Kadir Aslan and Chris D. Geddes*

DOI: 10.1039/b808292h

In this timely review, we summarize recent work on ultra-fast and sensitive bioassays based on microwave heating, and provide our current interpretation of the role of the combined use of microwave energy and plasmonic nanostructures for applications in rapid clinical and bioagent diagnostics. The incorporation of microwave heating into plasmonic nanostructure-based bioassays brings new advancements to diagnostic tests. A temperature gradient, created by the selective heating of water in the presence of plasmonic nanostructures, results in an increased mass transfer of target biomolecules towards the biorecognition partners placed on the plasmonic nanostructures, enabling diagnostic tests to be completed in less than a minute, and in some cases only a few seconds, by further microwave heating. The diagnostic tests can also be run in complex biological samples, such as human serum and whole blood.

Introduction

Historically, diagnostics has been a very competitive industry, where many companies and university research groups alike are continuously developing new products and techniques respectively, to meet the ever growing demand for faster, simpler and reduced cost diagnostic tests. For any new product to be competitive in the plethora of diagnostic products in use today, they need to meet or exceed several criteria already achieved by the current diagnostic tests: sensitivity, specificity, reproducibility and be relatively inexpensive. In addition, the rapidity of the diagnostic tests becomes an important issue in the event of an outbreak of an infectious disease or a biological terror attack that has immediate impact on human health.

Rapid diagnostic tests are usually employed in Point-of-Care (POC) devices,[1–5] where a qualitative visual assessment of the presence of relevant protein/analyte,[5,6] nucleic acids[7,8] or cells[9] is undertaken in a very efficient and simple flow system (lateral-flow or handheld assays).[10–12] More elaborate commercially available systems also incorporate microfluidic technology; significantly reducing the sample volume and the assay time to as little as 5–10 min.[13] However, these systems also require a relatively expensive initial investment on the equipment that is used to perform and read the diagnostic tests.[13]

Diagnostic tests are undertaken in two general formats: (1) ELISA (Enzyme-Linked ImmunoSorbent Assay),[14] and (2) fluorescence-based immunoassay.[15] In ELISA, an optical signal output is achieved after an enzymatic breakdown of a substrate and is read spectrophotometrically. Immunoassays (other than enzymatic ones) employ a variety of tag

Institute of Fluorescence, Laboratory for Advanced Medical Plasmonics, and Laboratory for Advanced Fluorescence Spectroscopy, Medical Biotechnology Center, University of Maryland Biotechnology Institute, 725 West Lombard St., Baltimore, MD, 21201, USA

Kadir Aslan

Dr Kadir Aslan is an Assistant Professor at the Institute of Fluorescence at the University of Maryland Biotechnology Institute (UMBI) studying the applications of plasmonics in medical biotechnology. He is the author of 70 papers and 10 book chapters.

Chris D. Geddes

Dr Chris D. Geddes, Professor, is internationally known in fluorescence spectroscopy and plasmonics, publishing over 175 papers and 15 books. He is the director of the Institute of Fluorescence at the University of Maryland Biotechnology Institute (UMBI), USA, and Editor-in-chief of both the Journal of Fluorescence *and the* Plasmonics Journal.

molecules such as fluorophores or in some cases gold nanoparticles due to their intense color in the visible range. Ultimately, a good rapid diagnostic test should have the speed and the simplicity of lateral-flow assays and the quantitative nature of ELISAs or fluorescence immunoassays. In this regard, current research around the world is focused on the amalgamation of optical detectors and simplified assay platforms, to develop new rapid diagnostic tests.[13]

Our research laboratory, The Institute of Fluorescence, at the University of Maryland Biotechnology Institute has recently both introduced and shown applications of several new approaches to rapid clinical diagnostic tests based on the combined use of low-power microwave heating with plasmonic nanostructures. These new approaches include: (1) solution-based aggregation assays;[16] (2) fluorescence-based surface assays[17–24] and (3) chemiluminescence-based surface assays[25–28] for the detection of small molecules, nucleic acids and/or proteins. In this timely review article, we summarize our previous work and present our current interpretation of the role of employing microwave heating in combination with plasmonic nanostructures as a new tool in rapid clinical and biodefense diagnostic tests and compare these technologies to current diagnostic challenges.

Microwave-accelerated nanoparticle aggregation assays (MA-AAs)

Plasmonic nanoparticles, especially gold nanoparticles, are frequently used in aggregation assays due to their exceptional optical and electronic properties.[29,30] When aggregated in solution, gold nanoparticles show a color change from an intense red color (for 20–40 nm and which also depends on size) to purple, indicative of surface plasmon coupling between the nearby nanoparticles.[29,30] This colorimetric response has been shown to have practical utility in DNA hybridization,[31,32] immunoassays,[33] small molecule sensing[29,34,35] and the monitoring of enzyme activity[36] by many research groups. Gold nanoparticles are also known to scatter light more efficiently than latex beads,[37,38] which has led to their use in scattering-based assays.[35,39] However, the rate-limiting step in the current nanoparticle aggregation assays is the time of the biorecognition, which typically takes as long as 30 min to complete.

In a recent paper,[16] it has been demonstrated that the incorporation of microwave heating to a gold nanoparticle aggregation protein assay can shorten the aggregation assay run time to *ca.* 10 s. Fig. 1(a) shows the *model* protein–nanoparticle aggregation assay, where 20 nm gold nanoparticles coated with biotinylated-BSA are aggregated in solution with the addition of streptavidin. Fig. 1(b) shows the absorption spectra of gold nanoparticles, which were similar after the addition of 20 nM streptavidin that was incubated at room temperature (no microwave heating – No Mw) for 20 min and microwave-heated for 10 s. On the other hand, no aggregation of nanoparticles was observed when the gold nanoparticles coated with biotinylated-BSA and streptavidin were incubated for 1 min at room temperature [Fig. 1(c)]. In addition, the gold nanoparticles did not

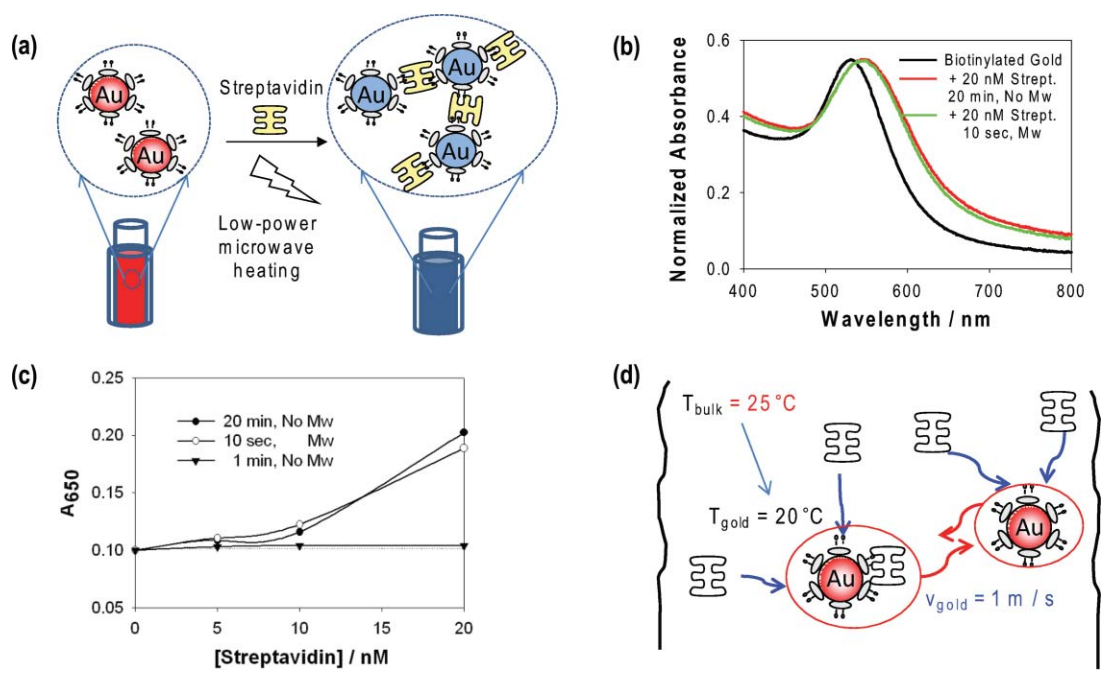

Fig. 1 Microwave-accelerated nanoparticle aggregation assays (MA-AAs) in solution. (a) Model protein–nanoparticle system used to demonstrate MA-AA in solution; biotinylated-BSA-coated 20 nm gold nanoparticles cross-linked by streptavidin. (b) Change in absorbance of biotinylated-BSA 20 nm gold nanoparticles cross-linked by 20 nM addition of streptavidin, both without (room temperature) and after low-power microwave heating. (c) Change in absorbance at 650 nm for both the room-temperature-incubated and microwave-heated samples. (d) Schematic representation of the aggregation process driven by a temperature gradient and kinetic energy of the nanoparticles. Mw – microwave heating. (Adapted with permission from ref. 16. Copyright 2007, American Chemical Society.)

aggregate when the biotin groups were omitted from the surface of the gold nanoparticles[16] (data not shown here). These results demonstrate that the aggregation assay was completed in *ca.* 10 s with low-power microwave heating, as compared to aggregation assays typically run at room temperature.

We summarize our explanation for the observations of faster aggregation times in Fig. 1(d): since metallic nanoparticles have high conductivity values, the electric and magnetic fields (from the microwaves) attenuate rapidly toward the interior of the metal due to the so-called 'skin effect'. This produces a force that pushes the conducting electrons towards an area adjacent to the boundary (skin depth), focusing the electric fields around the nanoparticles themselves. At 2.45 GHz (the conventional microwave frequency), the skin depth for gold nanoparticles lies within the micron range.[40] When the skin depth is larger than the dimensions of the metal particles themselves, the effect is negligible. Thus, for gold nanoparticles, the microwave heating is uniform throughout the dimensions of the nanoparticle but low. It was previously calculated that the temperature increase around the gold nanoparticles due to microwave heating is in the order of a few microKelvin.[16,40] That is, gold nanoparticles remain at the same temperature before the microwave heating is initiated. On the other hand, water is known to significantly absorb microwave energy at 2.45 GHz and is subsequently heated more efficiently as compared to gold nanoparticles.[41] As a result, a temperature gradient is created between the water and the gold nanoparticles due to the selective heating of water. The temperature gradient subsequently drives the proteins (present in water) towards the colder gold nanoparticles whilst under microwave heating, *cf.* Fig. 1(d). In the mean time, the gold nanoparticles dissipate the absorbed microwave energy as kinetic energy (an increased velocity, see the supporting information in ref. 16 for velocity calculations) and then, combined with the temperature gradient effect, result in much faster aggregation times, *i.e.* reduced assay run times. It is very important to note that proteins are not directly heated by the microwave energy, as their dielectric absorption occurs in the MHz frequency range[41] and thus are not denatured in the process. It is also important to comment on the existence of the temperature gradient in view that the thermal conductivity for gold (317 W m^{-1} K^{-1}) is significantly larger than that of water (1.05 W m^{-1} K^{-1}). After the onset of microwave heating the average temperature of the bulk medium is increased by *ca.* 5 °C for 10 s of microwave heating. For the duration of the microwave heating (10 s), as heat is transferred from the bulk water to gold, and the temperature on the surface of the gold nanoparticles reaches an equilibrium temperature lower than the bulk, water molecules are continuously circulated between the warmer and the colder regions of the bulk medium.

In summary, this approach has some significant advantages for biosensing, including:

(1) bioassays can be kinetically completed within only a few seconds;

(2) the technology is applicable to all current nanoparticle-based assays;

(3) the biological materials are not denatured by low-power microwave heating.

Microwave-accelerated metal-enhanced fluorescence (MAMEF)-based protein assays on planar substrates

Most rapid clinical and bioagent diagnostic tests are run on a solid surface allowing the subsequent separation of unwanted assay components after the completion of the relevant assay steps. In a recent surface assay technique, named microwave-accelerated metal-enhanced fluorescence (MAMEF),[17] the use of low-power microwave heating is combined with metal-enhanced fluorescence to both kinetically accelerate the biorecognition events and to simultaneously increase the fluorescence readout, *i.e.* enhance the analyte detection limit.

The proof-of-principle of the MAMEF technique was demonstrated with a model protein–fluorophore system,[17] biotinylated-BSA and fluorophore-labeled streptavidin, as shown in Fig. 2(a). The biotin–streptavidin biorecognition event takes up to 30 min to complete at room temperature on the assay surface (>95%), while low-power microwave heating reduces the assay run time to an attractive 20 s. The assay was constructed on a glass microscope slide (other materials such as paper,[42] plastics,[43] HTS wells,[20] *etc.*, can also be used) coated with silver nanoparticles, with an approximate 40% surface coverage [Fig. 2(b)]. In this surface configuration, the use of silver nanoparticles results in (1) enhancement of fluorescence as compared to a blank glass surface (increased emission), and (2) creation of a temperature gradient between the bulk and the silver nanoparticles themselves. For 2 s of microwave heating of water on a blank glass slide and glass slides coated with silver nanoparticles, the temperature increase is [measured using a thermal camera, Fig. 2(c)] 0.5 and 2 °C, respectively.[44] The temperature of water on a glass slide coated with silver nanoparticles increases by 5 °C for a 20 s low-power microwave heating[17] (data not shown here).

Fig. 3(a) shows the schematic representation of a MAMEF-based surface protein detection assay. In MAMEF, while water is selectively heated with microwaves the silver nanoparticles remain virtually at the same temperature as they were before the microwave heating is initiated. The selective heating of these assay components creates a temperature gradient between the water and the glass and silver nanoparticles, which results in the transfer of streptavidin molecules from the warmer bulk to the colder surface due to temperature-driven mass transfer. Since the thermal conductivity of silver (429 W m^{-1} K^{-1}) is much larger than that of glass (1.05 W m^{-1} K^{-1}), the transfer of streptavidin happens more efficiently towards silver nanoparticles on glass than to the unsilvered region of the glass. For the duration of the microwave heating (20 s), as heat is transferred from the bulk to the surface, and the temperature on the surface of the silver nanoparticles reaches an equilibrium temperature lower than the bulk, water molecules are continuously circulated between the warmer and the colder regions of the bulk medium.

It is also important to note that, in this particular surface assay, there is also a permanent concentration gradient (for streptavidin molecules) between the bulk and the glass surface: the concentration of fluorophore-labeled streptavidin is 10 μM and is significantly larger than the concentration of biotinylated-BSA on the glass surface (estimated to be in the nanomolar range). The concentration of streptavidin molecules is still approximately micromolar even after the assay is completed. The evidence for the processes described above

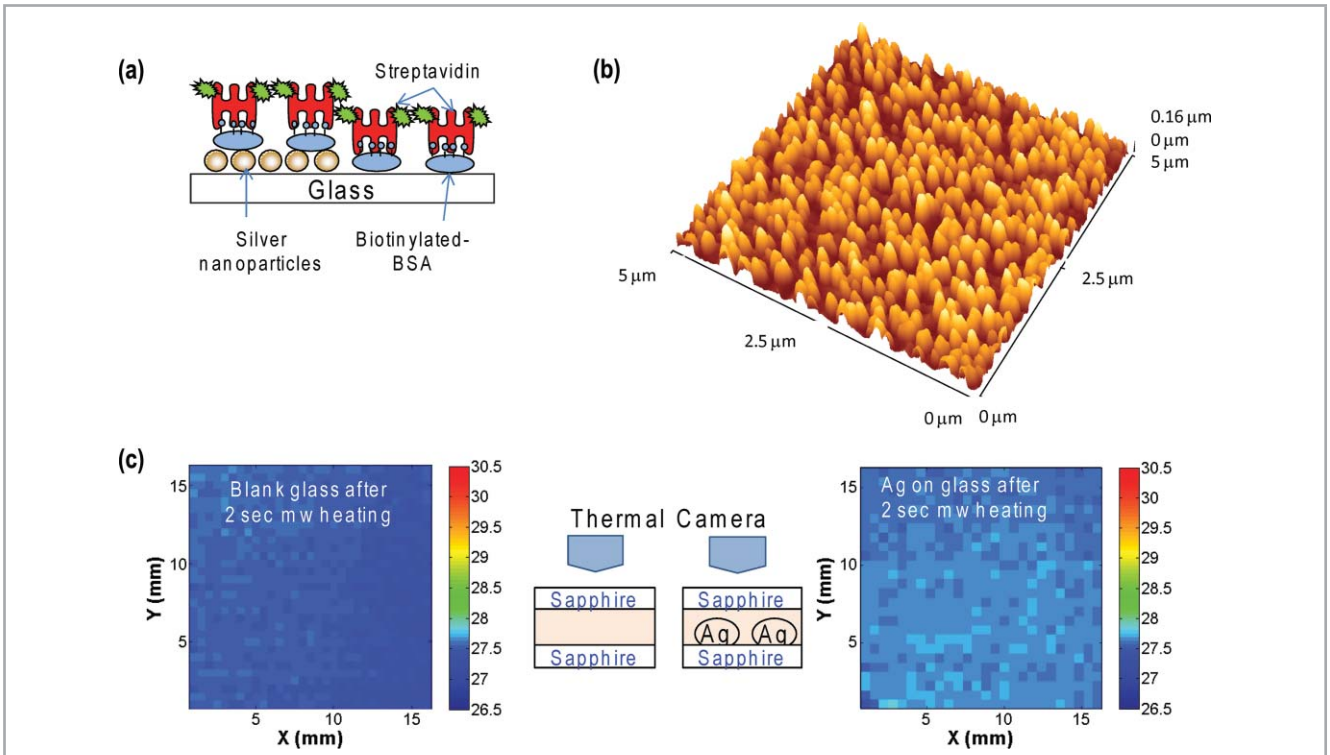

Fig. 2 MAMEF-based surface assays. (a) Model protein–fluorophore system used to demonstrate MAMEF on glass substrates. (b) Atomic Force Microscope (AFM) image of silver island films (SIFs) deposited onto glass. (c) Real-time temperature distributions of water on a blank and SIFs-deposited sapphire substrates captured using a thermal camera. The cartoon shows the arrangement of the surfaces in the experimental setup. (Adapted with permission from refs 17 and 44. Copyright 2005, American Chemical Society; copyright 2007, Springer.)

can be seen from the fluorescence emission spectra in Fig. 3(b) and 3(c). Similar fluorescence emission spectra from the fluorophore (FITC)-labeled streptavidin were measured after the surface assay was completed at room temperature [RT; 30 min, Fig. 3(c)] or with microwave heating [Fig. 3(b)]. Fig. 3(b) and 3(c) also show that the assay run on the blank glass slide with microwave heating did not go to completion, since the emission intensity is significantly less than the assay run at room temperature. This observation alone shows the importance of silver nanoparticles, which provide the means for the creation of the temperature gradient.

In the context of diagnostics, the MAMEF technique is particularly attractive as it provides for (1) enhanced fluorescence signatures, *i.e.* lower analyte concentration detectability due to metal-enhanced fluorescence (MEF);[45] (2) very rapid assay kinetics and (3) protection against surface protein denaturation, as the metalized surfaces are colder than the bulk medium, and therefore protect against thermal denaturation.

Microwave-accelerated metal-enhanced fluorescence (MAMEF)-based DNA hybridization assays on planar substrates

Fluorescence is also one of the most commonly used technologies in DNA hybridization assays. In DNA hybridization assays performed on planar substrates, an anchor probe that is attached to a planar surface is hybridized with a target oligonucleotide from a sample and a fluorescent probe added into the hybridization media. The fluorescence readout is directly related to the amount of target oligonucleotide present in the sample used. The application of the MAMEF technique to DNA hybridization assays has recently been shown.[21,22,24] One particular notable application is a MAMEF-based three-piece DNA hybridization assay for the detection of *Bacillus anthracis* (anthrax)[24] [Fig. 4(a)]. In this assay, an anchor probe with a specific oligonucleotide sequence that recognizes target anthrax DNA is attached to silver nanoparticles *via* a thiol bond. The non-specific binding of DNA to the assay platform silver nanoparticles and glass is modified with additional surface-protective chemicals. A sample containing the exosporium of anthrax and the exosporium of its non-virulent close relative *Bacillus cereus* is mixed with a fluorescent probe (also hybridizes along a different region of anthrax DNA) and is hybridized on the silvered surface with low-power microwave heating for *ca.* 30 s. Also, a control experiment where the anchor probe is omitted from the silver surface was also performed, with the results shown in Fig. 4(b–d). Fluorescence emission intensity at 585 nm from this control assay shows a constant emission intensity while the regular assay shows an increase in emission intensity over a wide range of concentrations, indicating that the MAMEF assay platform can clearly detect the target anthrax exosporium DNA in the presence of DNA from a non-virulent strain of anthrax. It is important to note that each data point was measured from a separate experiment at the same collection times. While Fig. 4

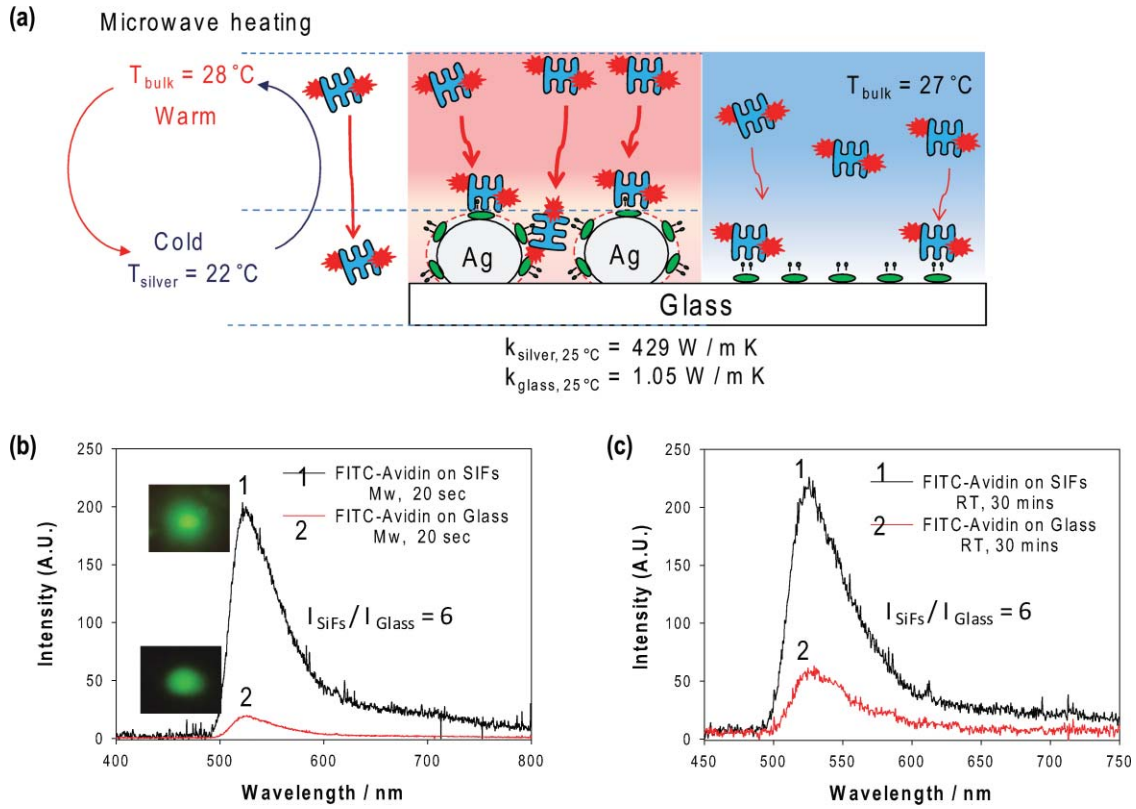

Fig. 3 A model MAMEF-based protein detection assay. (a) Schematic representation of the effect of microwave heating on the protein detection surface assay: while water is selectively heated with microwaves, silver nanoparticles remain at the same temperature as before the microwave heating is initiated. Emission spectra of a fluorophore (FITC) for a model protein assay run: (b) with microwave heating for 20 s and (c) at room temperature for 30 min. Real-color photographs taken through an emission filter are also shown as visual conformation of enhanced fluorescence observed due to the presence of silver nanoparticles. FITC – fluorescein isothiocyanate; RT – room temperature; SIFs – silver island films. (Adapted with permission from ref. 17. Copyright 2005, American Chemical Society.)

and recent work has been focused at anthrax detection,[24] the approach clearly demonstrates that the three-piece DNA MAMEF assay concept could readily be applied to the detection of virtually any DNA target. Interestingly, this approach has also been applied to the detection of an RNA 500-mer,[46] as an alternative technology to the laborious Northern Blot approaches.

Microwave-triggered metal-enhanced chemiluminescence (MT-MEC) assay on planar substrates

Plasmonic nanoparticles have also been shown to couple to the chemically excited state of lumophores and subsequently enhance chemiluminescence emission, a phenomenon named metal-enhanced chemiluminescence (MEC) by Geddes and co-workers.[47,48] It has also been shown that when exposed to microwave energy, the reactions that result in chemiluminescence emission can be additionally 'triggered' and also driven to completion within seconds.[25] This diagnostic technology is named microwave-triggered metal-enhanced chemiluminescence (MT-MEC). In MT-MEC, while the silver nanoparticles increase the chemiluminescence emission (plasmon enhancement), microwave energy shortens the detection times of the chemiluminescence emission (blue, green and red), even in the absence of silver nanoparticles, by rapidly accelerating the chemiluminescence kinetics.[25]

The proof-of-principle application of the MT-MEC technique to protein detection assays has also been demonstrated[27] [Fig. 5(a)]. In the MT-MEC protein detection scheme, biotinylated-BSA is incubated with horseradish peroxidase (HRP)-labeled streptavidin on a glass microscope slide coated with silver nanoparticles. Half of the glass support slide was left blank (control sample) to investigate the effect of the silver nanoparticles on chemiluminescence. Fig. 5(b) shows the chemiluminescence emission as a result of enzymatic activity from the blank glass slide collected over a 500 s time period. The sample is also subjected to 30 s microwave pulses twice, during which a significant increase in chemiluminescence emission is observed, demonstrating the effect of microwave heating on chemiluminescence reactions, *i.e.* they are enhanced due to the accelerated diffusion of the reactants.[27] When the identical protein detection assay was run on glass slides coated with silver nanoparticles, an increase in chemiluminescence emission (*ca.* three-fold) was observed [Fig. 5(c)]. When subjected to low-power microwaves, the chemiluminescence emission from the silver nanoparticles is further enhanced for the microwave pulse

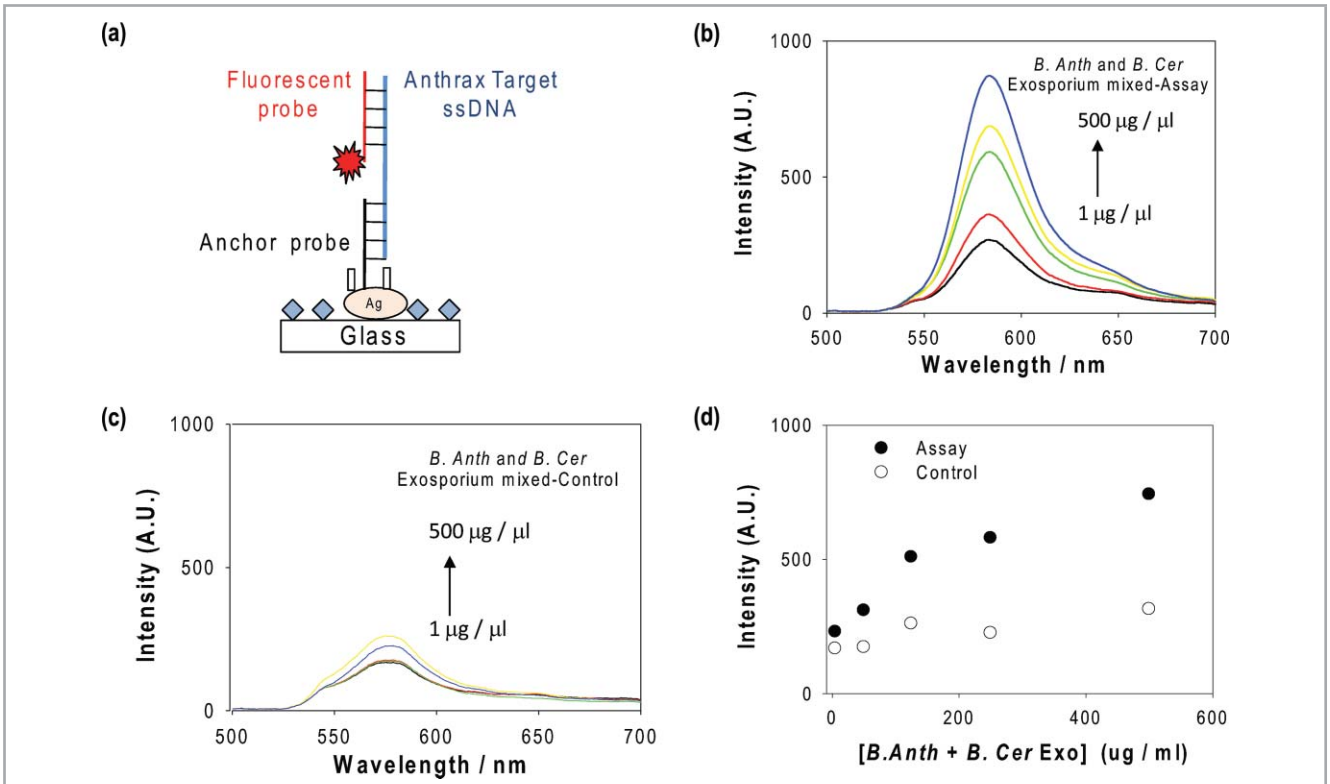

Fig. 4 MAMEF-based anthrax DNA hybridization assay on silvered glass substrates. (a) Experimental design, depicting the organization of the DNA oligomers on SiFs used for the detection of *B. anthracis*. Emission spectra of fluorophore (TAMRA)-labeled ssDNA as a function of concentration: (b) of a mixture of samples containing *B. anthracis* and *B. cereus* after 30 s low-power microwave heating and (c) the corresponding control experiment where the anchor probe is omitted from the surface. (d) Semi-logarithmic plot of the fluorescence emission intensity at 585 nm for the TAMRA-ssDNA [from (b) and (c) as a function of the target DNA concentration]. TAMRA – tetramethylrhodamine; ss – single stranded; SIFs – silver island films. (Adapted with permission from ref. 24.)

time intervals. These results show the 'on-demand' nature of microwave-triggered chemiluminescence reactions, where one can drive these reactions to completion when desired, using microwave heating. Fig. 5(d) shows a plot of photon flux (overall counts collected over 500 s for each data point) for different concentrations of biotinylated-BSA from the MT-MEC assay run on both glass and silvered surfaces. It is believed that the use of silver nanoparticles serves an important purpose in the MT-MEC technique: chemiluminescence emission is enhanced due to close proximity of these reactions to silver nanoparticles (MEC).[48] The reader is referred to the literature for further information regarding the mechanism for MEC.[47,48] We envision that the MT-MEC technique can be implemented into standard protein detection methodologies where ultra-fast, sensitive and low-cost chemiluminescence assays can be realized.

One particular advantage of the MT-MEC technique lies in the fact that bursts of photons are triggered on demand. While the collection of more photons directly translates to a better assay sensitivity, the reduced chemiluminescence glow times eliminate the long 'slow-glow' associated with chemiluminescence-based diagnostics. *For the first time*, chemiluminescence-based assays can now be used as a rapid (<1 min) diagnostic tool.

Microwave-focused chemiluminescence (MFC) for the detection of proteins on planar substrates

As described in the previous section, the MT-MEC technique offers an alternative to chemiluminescence-based protein assays run on planar surfaces. In MT-MEC, the 'trigger' effect by microwaves is limited to a small region in close proximity to the plasmonic nanoparticles where the enzymatic activity and plasmon optical enhancement takes place. Thus, for a detectable chemiluminescence readout, a region (as small as 5 mm) on the assay surface has to be coated with the nanoparticles regardless of the method of deposition (either random or in an ordered fashion). It has been shown that the enzyme-catalyzed chemiluminescence reactions *cannot* be 'triggered' in solution away (distal) from the silvered surface.[27] Moreover, one has limited control over the temperature of the assay bulk media. The lack of spatial and temporal control in MT-MEC subsequently limits the application of this technique only to surface assays, within 100 nm of the nanoparticles.

However, a new technology was recently introduced, named microwave-focused chemiluminescence (MFC),[49] to 'trigger' chemically- and enzyme-catalyzed chemiluminescence reactions with spatial and temporal control, directly addressing some constraints of the MT-MEC technique. In MFC, the plasmonic nanoparticles are replaced with millimeter-sized aluminium structures (mini-antennas) which focus the incident electric field to the

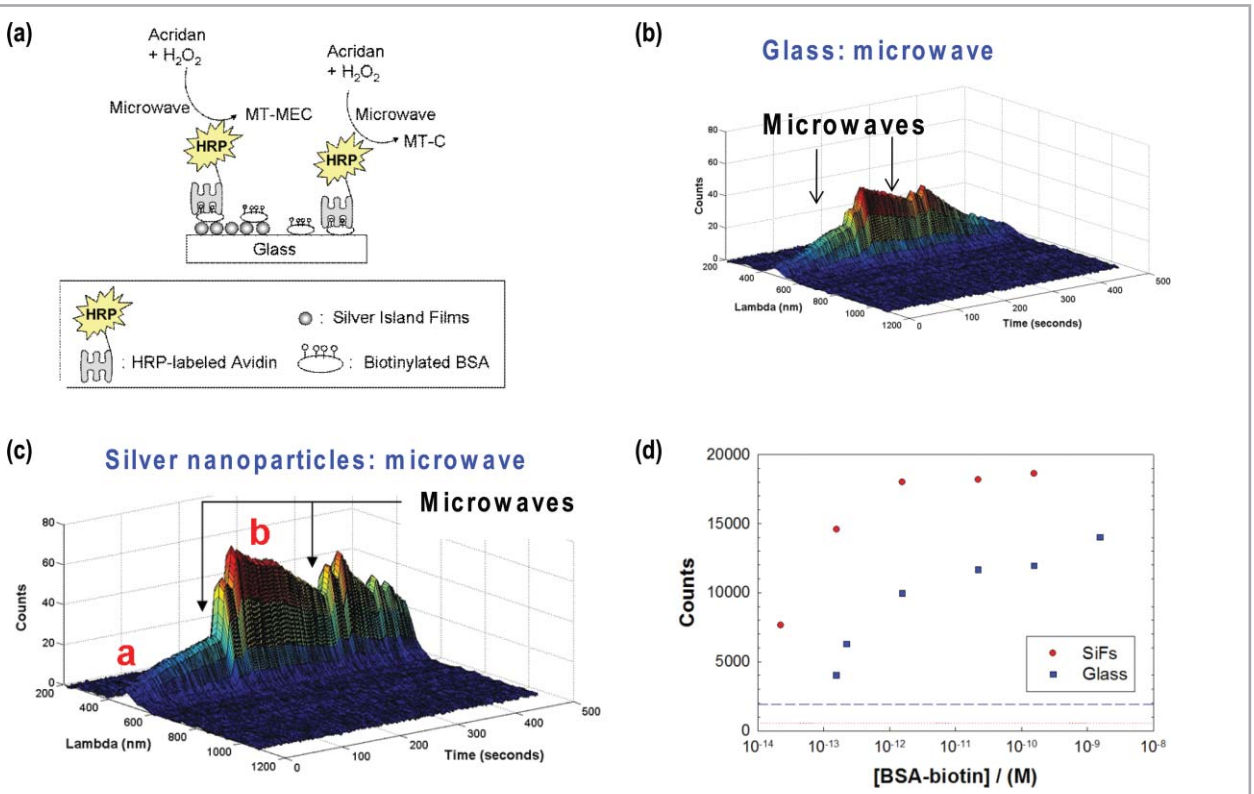

Fig. 5 Microwave-triggered metal-enhanced chemiluminescence (MT-MEC) assay on planar substrates. (a) Experimental design, depicting the MT-MEC assay on both glass and silvered slides. Plots of acridan emission as a function of time: from (b) glass slides and (c) silver nanoparticle-deposited glass slides with low-power microwave heating. (d) Photon flux (in counts) for different concentrations of BSA-biotin from both glass and silvered surfaces. Baselines (straight dashed and dotted lines) correspond to integrated photon flux for glass and silvered surfaces incubated with 1% BSA solution and streptavidin-HRP. HRP – horseradish peroxidase; SIFs – silver island films. (Adapted with permission from ref. 27. Copyright 2006, American Chemical Society.)

tip and/or the corners of the structures. One interesting mini-antenna design is the so-called disjointed 'bow-tie' design, where two equilateral aluminium triangles are separated by a small gap distance (up to several mm). Fig. 6(a) shows the finite-difference time-domain (FDTD)-based simulation of electric field distributions for two aluminium 12.3 mm triangle structures in a 2.45 GHz microwave field. These simulations are complex numerical simulations and solutions to Maxwell's equations for the propagation of electromagnetic fields on complex structures. This configuration, in theory, short-circuits the propagation of the microwave field TFSF (total-field scattered-field) source across the metal surface in such a way that electric charge builds on the tips of the aluminium triangles adjacent to the gap and the electric field between the aluminium structures is strongly enhanced [Fig. 6(a)]. FDTD simulations allow one to simulate the total electric field distributions for different gap sizes [Fig. 6(b)]. A gap size of 0.05 mm can yield up to a 50 000-fold increase in electric field intensity, which diminishes for larger gap sizes, as compared to another point in the geometry.

In order to demonstrate that regions of maximum electric field enhancements predicted by FDTD simulations for 'bow-tie' aluminium structures correlate well with maximum chemiluminescence enhancements, studies were undertaken as shown in Fig. 6(c)-top. In the experiment, a chemiluminescent solution was placed in the gap between the aluminium structures and exposed to short, low-power microwave pulses. Fig. 6(c) shows that the chemiluminescence intensity from the material is increased *ca.* 500-fold by microwaves, demonstrating that the simulated electric field distributions can be used as a predictive tool to spatially control and map chemiluminescence-based reactions. It was also shown that single aluminium triangles focus the electric field around the tips.[49] Fig. 6(d) shows the acridan chemiluminescence emission as a function of time from HRP-modified glass coverslips coated with 1 μM BSA-biotin and 1 mM HRP-streptavidin and positioned glass substrate geometries with and without aluminium triangles, experimentally confirming the predictions made by FDTD simulations.

Since the enhanced electric field predicted by FDTD simulations persists in the *z*-direction (well into the bulk of a solution), one can also re-use the aluminium structures by carrying out the surface assays on a disposable glass slide (or coverslip) placed on top of the aluminium structures.[49] Fig. 6(c)-bottom shows the experimental configurations of the model surface protein assay performed on a disposable coverslip placed over various

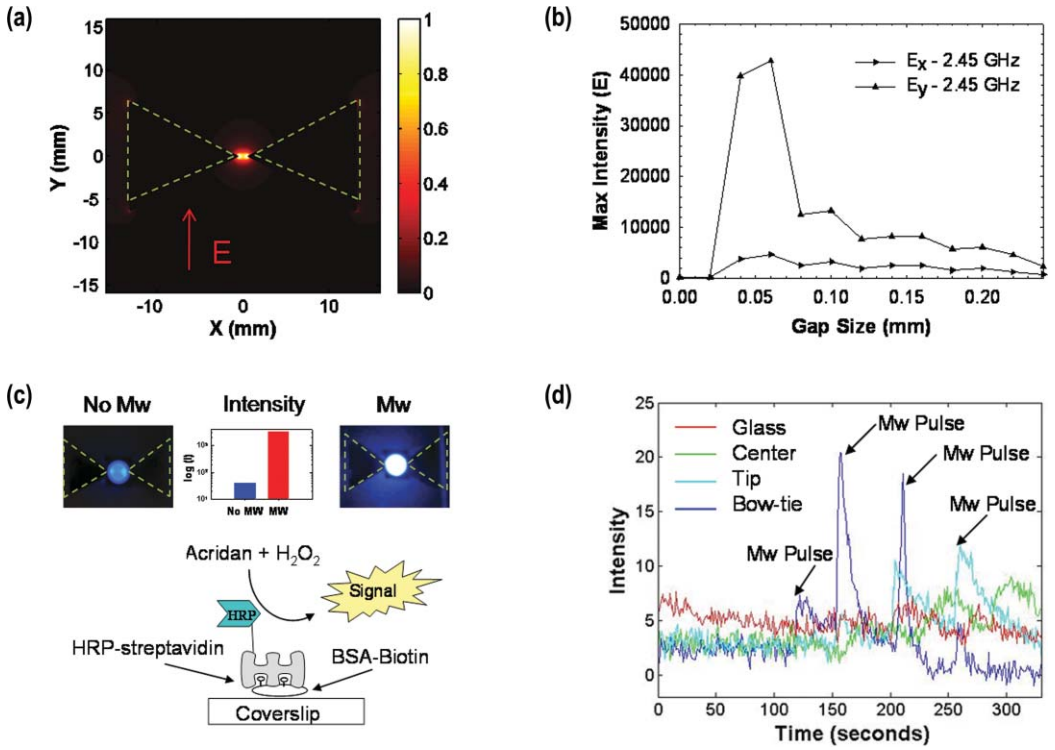

Fig. 6 Microwave-focused chemiluminescence (MFC) for the detection of proteins. (a) Normalized FDTD simulation of field intensity distributions $[I_x(E_y^2) + I_y(E_y^2)]$ for equilateral aluminium triangles in a simulated 2.45 GHz transverse electric polarized total-field scattered-field that propagates across the geometries from bottom to top (z-direction). (b) Maximum I $[I_x(E_y^2) + I_y(E_y^2)]$ pixel intensity *versus* gap size for the equilateral triangle configurations. (c) Chemiluminescence measured both before (blue bar) and after (red bar) the application of the low-power microwaves from glass substrates modified with vapor-deposited aluminium triangles; model BSA-biotin, HRP-streptavidin chemiluminescent assay scheme. (d) Acridan chemiluminescence emission as a function of time from HRP-modified glass coverslips coated with 1 μM BSA-biotin and 10 ng HRP-streptavidin and positioned glass substrate geometries with and without aluminium triangles. (Adapted with permission from ref. 27. Copyright 2006, American Chemical Society.)

structures: glass or aluminium. Without microwave heating, 'steady-glow' from all sample geometries can be seen (0–100 s) [Fig. 6(d)]. After the initiation of microwave heating, 'triggered' chemiluminescence emission can only be observed from sample geometries that employ aluminium structures.[49] In addition, the chemiluminescence emission is depleted using only the bow-tie sample geometry within 100 s, demonstrating the effectiveness of these aluminium structures in 'triggering' chemiluminescence emission.

In terms of diagnostics, the MFC technology has some *significant benefits* over current chemiluminescence-based approaches:

(1) the enhanced chemiluminescence signatures can be spatially modeled using FDTD approaches;

(2) chemiluminescence enhancements up to 50 000-fold have been demonstrated;[49]

(3) the technology uses current chemiluminescence substrates;

(4) the chemiluminescence can be 'triggered' on demand with very high photon fluxes in a short period of time.

Microwave-accelerated surface plasmon-coupled luminescence (MA-SPCL) for protein and DNA detection

Surface plasmon fluorescence spectroscopy (SPFS), a technique that utilizes the efficient coupling of fluorescence emission with the surface plasmons of metallic surfaces, was fully demonstrated by Knoll[50,51] in 1999. One can also find several observations describing the metal–fluorophore interactions.[52–55] In SPFS, fluorophores chemically attached to biomolecules placed in close proximity to thin metal films are exposed to strong fields resulting in enhanced fluorescence that is highly polarized and directional.[50] The emitted fluorescence photons that are dependent on the concentration of an analyte on the surface can subsequently be monitored. This mode of detection has been shown to significantly increase the sensitivity of bioassays.[51] However, one does not have control over the assay run time. In this regard, a recently introduced technique named microwave-accelerated surface plasmon-coupled luminescence (MA-SPCL),[23] that combines the use of microwave heating and SPFS to develop ultra-fast and sensitive bioassays, significantly alleviates this problem. In the MA-SPCL technique, low-power microwave heating affords for the kinetic acceleration of biorecognition reactions (even in complex biological media) and the surface plasmon-coupled fluorescence increases the optical sensitivity of the assays undertaken. It is this unique combination that makes the MA-SPCL technique a

powerful alternative to current rapid diagnostic tests.[56]

Since MA-SPCL employs thin plasmonic films, FDTD simulation techniques can again be used to predict the interactions of microwaves with the assay sample geometry. Fig. 7(a) shows the FDTD calculations for electric field distributions of a 2.45 GHz microwave field incident on a gold disk (5 mm in diameter and 50 nm thick). The scale bar (electric field distribution) represents the effectiveness of heating the sample. The FDTD simulations predict that the assay media proximal to the edges of the rotating gold disk in the microwave cavity will be effectively heated. In addition, assay media above the gold disk will be selectively heated with microwaves, whereas the gold disk will not be heated itself. The differences in the extent of heating of the assay media and the gold disk creates a temperature gradient (warmer assay media, colder gold assay surface), which affords for the kinetic acceleration of biorecognition events in close proximity.

Fig. 7(b) shows the change in average temperature (ΔT) of the sample captured using a thermal imaging camera during microwave heating of the sample. The average temperature of the bulk solution on a plain glass surface increases by 1 °C for a 2 s microwave pulse [Fig. 7(b)-top left; Mw heating was turned ON and OFF] and does not cool for the remainder of the microwave heating process. This implies that the temperature of the glass surface and the bulk solution reaches a thermal equilibrium (no temperature gradient). On the other hand, the average temperature of the bulk solution, only above the gold disk, increases by 0.5 °C for a 2 s microwave pulse and then starts to decrease immediately after the microwave pulse is turned off, due to cooling. The average temperature of the whole system (glass, gold disk and bulk solution) shows a similar heating/cooling trend to that of a gold disk with a more apparent cooling process. The observed cooling process, which is attributed to the temperature gradient created by the selective heating of the bulk solution over the gold disk (not heated with microwaves), indicates that there is an associated mass transfer (of biological materials in the bulk solution) from the warmer regions to colder regions of the assay surface.

In two recent papers,[23,57] the application of the MA-SPCL technique for the detection of proteins and DNA in human serum and whole blood has been shown. Fig. 8(a) shows the optical setup used for MA-SPCL-based bioassays. In SPCL, a gold disk is attached to a hemispherical prism with an index-matching fluid and this combined sample assembly is placed on a platform where the SPCL measurements are performed. The sample is excited from the sample side with a laser of choice at an angle of 90° (to the metal film). In this sample geometry, the fluorescent species are excited from the air side and the coupled fluorescence emission is then detected from the prism side. This configuration also allows the detection of free-space emission from the air side. The observation of the surface plasmon-coupled emission between the angles of 180 and 360° is performed from the prism side. The gold disk affords for directional emission at two specific angles (217 or 315°) [Fig. 8(b)]. Owing to the imperfections in the experimental setup one notes a slight difference in the angles of directional emission, which are expected to occur at the same angles symmetric to 270°. Fig. 8(b) shows a similar angular distribution of surface plasmon-coupled emission and free-space emission for a model protein (biotinylated-BSA/streptavidin) detection assay run both with microwave heating and at room temperature.[23] The biotin–streptavidin assay that takes up to 30 min at room temperature can be completed within 1 min using microwave heating, a 30-fold increase in assay kinetics.

The benefits of the MA-SPCL technique for assays run in complex media such as human serum and whole blood was also demonstrated by repeating the

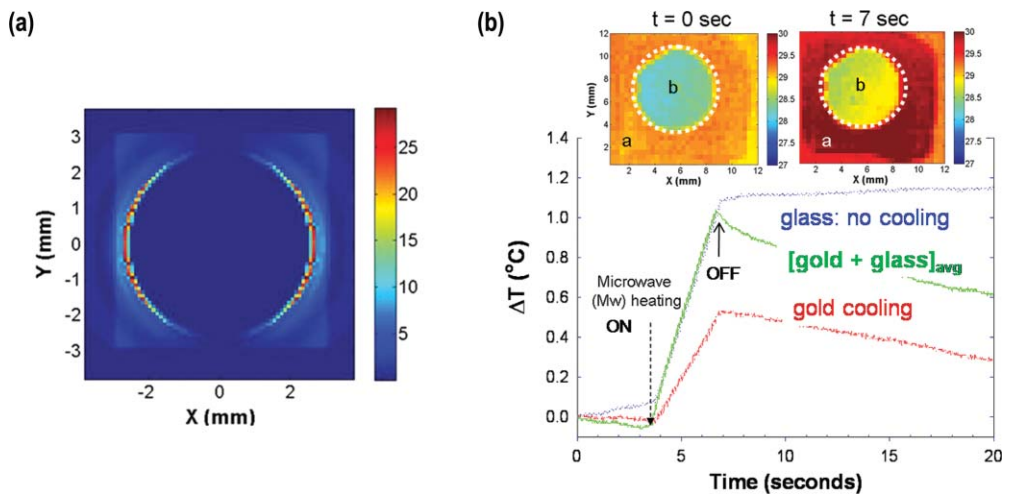

Fig. 7 Microwave-accelerated surface plasmon-coupled luminescence (MA-SPCL). (a) Finite-difference time-domain (FDTD) calculations for a gold disk of 5 mm diameter in a 2.45 GHz microwave field depicting the electric field distributions around the gold disk. (b) The change in average temperature (ΔT) of the sample as captured using a thermal imaging camera during microwave heating. The insets show snapshots of the thermal images of the sample geometry before ($t = 0$ s) and during ($t = 7$ s) microwave heating. (Adapted with permission from ref. 51. Copyright 2000, Elsevier.)

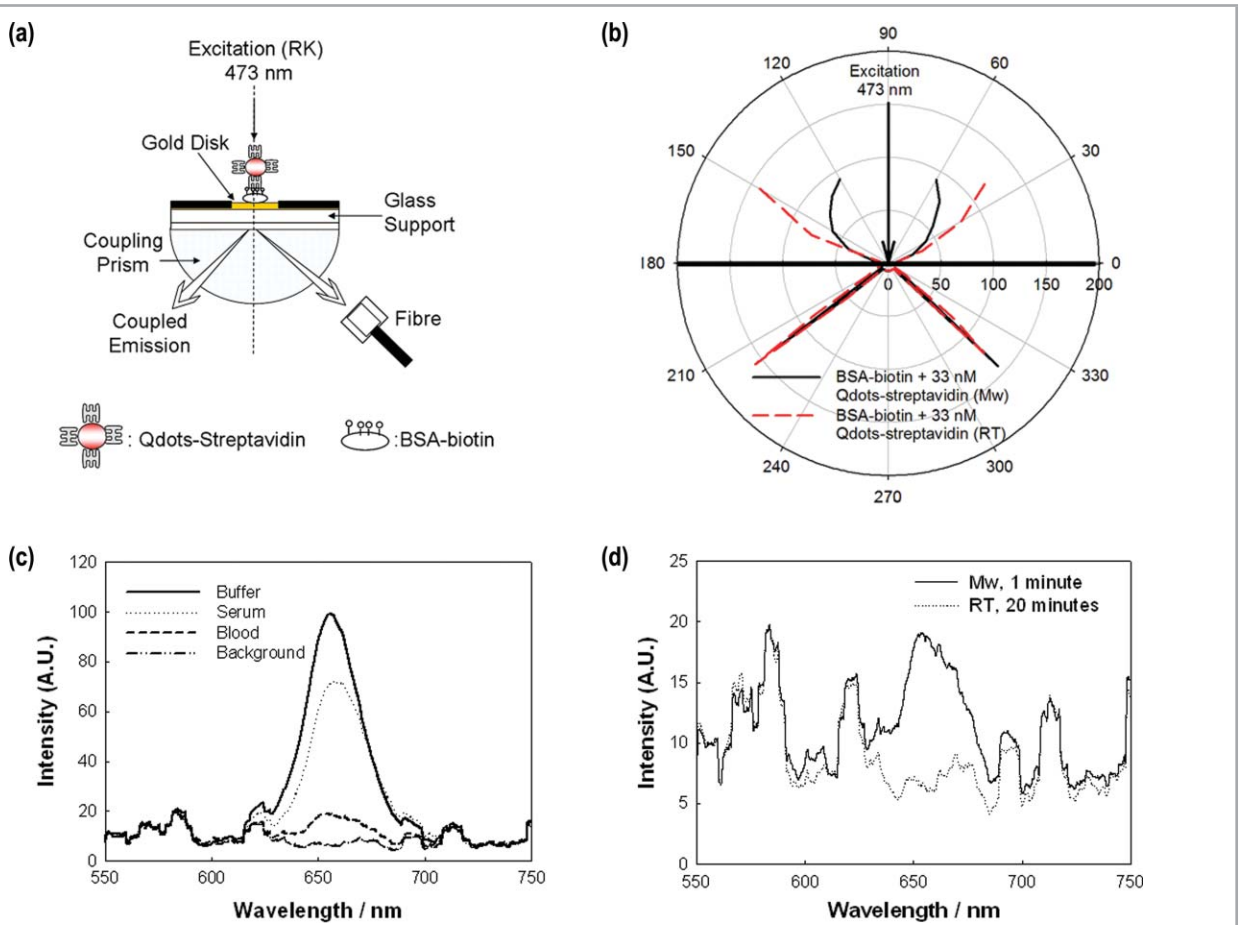

Fig. 8 Microwave-accelerated surface plasmon-coupled luminescence studies for the detection of proteins. (a) Optical setup for microwave-accelerated surface plasmon-coupled luminescence (MA-SPCL) bioassays. The sample is excited directly in the reverse Kretschmann (RK) configuration. (b) Angular distribution of luminescence for 33 nM of quantum dots–streptavidin used in the MA-SPCL assay, both microwave-heated (Mw) and run at room temperature (RT). (c) The emission spectra for 33 nM quantum dots used in the MA-SPCL assay measured at 217° in different media. (d) The MA-SPCL assay (Mw, 1 min) and the SPCL assay at room temperature (RT, 20 min) performed in whole blood measured at 217°. The angles are defined against the metal films. (Adapted with permission from ref. 23. Copyright 2007, Elsevier.)

model protein assay in buffer, serum and whole blood with microwave heating and at room temperature [Fig. 8(c) and 8(d)]. Fig. 8(c) shows the comparable intensity of surface plasmon-coupled emission measured from buffer and serum. Interestingly, the MA-SPCL assay still yielded a measurable signal (one-fifth of that of the buffer) with a signal-to-noise ratio of >3 (considered acceptable for fluorescence-based assays). The real advantage of the MA-SPCL technique for whole blood assays becomes apparent when it is compared to the whole blood assay run at room temperature [Fig. 8(d)]. While the model protein assay run in whole blood microwave accelerated yielded a measurable signal, the identical assay run at room temperature did not yield any signal due the coagulation of blood after several minutes. It is important to comment on the spectral features seen in Fig. 8(c) and 8(d): in these experiments, the emission peaks of commercially available quantum dots at 655 nm are clearly observed as compared to the background signal (no quantum dots). The background spectrum [Fig. 8(c)] displays several other peaks at wavelengths other than 640–670 nm, which were identical in all measurements. Since the intensity of these peaks was constant in all measurements, the emission peak observed at 655 nm is that of the quantum dots. In the MA-SCPL technique, microwave heating prevented the entrapment of assay components (especially fluorophore-labeled biological materials) due to the rapid assay run times (faster than the coagulation of blood).

In another recent paper,[57] the application of the MA-SPCL technique to DNA hybridization assays has been demonstrated. Fig. 9(a) shows the experimental design depicting the organization of Hepatitis C-specific oligomers on the assay surface as well as the sequence of the oligomers themselves. The detection of surface plasmon-coupled emission was performed using the same experimental setup as shown in Fig. 8(a). Fig. 9(b) and 9(c) show the concentration-dependent emission intensity values for assays run with microwave heating (1 min) and at room temperature (4 h), respectively. Both assays yield similar final emission intensities for all the concentrations. In control experiments undertaken with microwave heating, where the anchor probe is omitted from the surface, little or no detectable

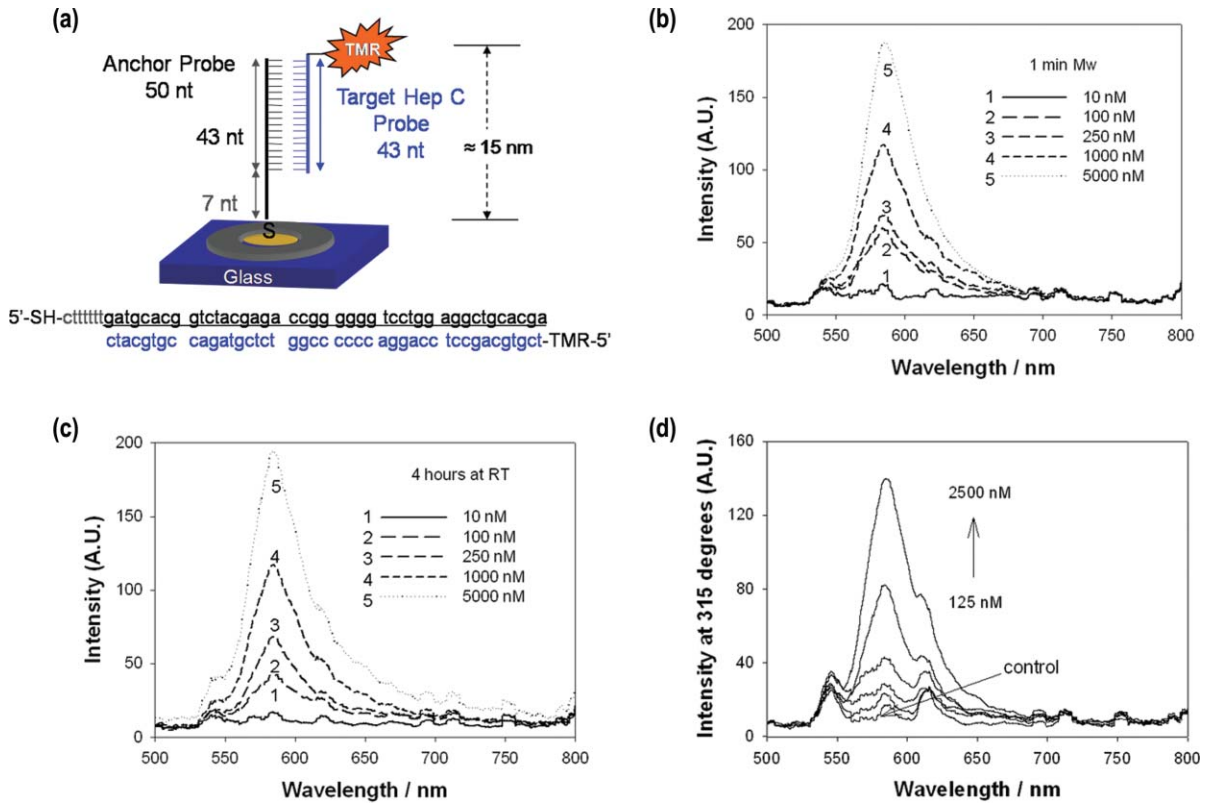

Fig. 9 Microwave-accelerated surface plasmon-coupled luminescence studies for DNA hybridization. (a) Experimental design depicting the organization of the DNA oligomers on gold disks used for the detection of the model Hepatitis C (Hep C) assay. The Hep C-specific oligonucleotide sequences are also given. The emission spectra of varying concentrations of TAMRA-labeled target DNA used in the (b) MA-SPCL assay (buffer), (c) at room temperature (RT, buffer) and (d) MA-SPCL run in whole blood. (Adapted with permission from ref. 51. Copyright 2000, Elsevier.)

signal was observed (not shown here), indicating the effectiveness of microwave heating in significantly reducing the non-specific binding events. The applicability of the MA-SPCL technique to DNA hybridization assays run in whole blood was also demonstrated by repeating the identical assay in Fig. 9(b) and 9(c). Fig. 9(d) shows that the concentration-dependent emission spectra measured from whole blood samples are similar to those measured from samples in buffer. In the control experiment, the emission intensity from a sample containing a high concentration of oligonucleotide was measured to be less than that of all the samples used in the regular assay, once again providing additional evidence for the effectiveness of microwave heating for ultra-fast bioassays.

In the context of diagnostics, the MA-SPCL technique has much to offer:

(1) a metallic thin film surface architecture, which is both easily fabricated and inexpensive;

(2) the SPCL emission is highly directional from the back of the films, affording for sensitive analyte detection;

(3) the assays can be operated in both a Kretschmann and reverse Kretschmann configuration. For whole blood samples, the shallow penetration of the surface evanescent field[58] affords for high sensitivity detection;

(4) the assays can be kinetically completed in <30 s;

(5) the gold disks are re-usable, although other metals can be used in different wavelength regions;

(6) the MA-SPCL approach uses moderately inexpensive and readily available fluorescence components and therefore could be potentially amalgamated into existing diagnostic devices.

Summary and future outlook

Current rapid clinical and bioagent diagnostic tests are available, either as hand-held devices (lateral-flow assays) that are designed to qualitatively indicate the presence of an analyte of interest within a few minutes, or as part of a more complex system that allows the quantitative assessment of samples using expensive optical instruments and other parts.[56] While handheld devices are simple and relatively inexpensive, the fact that the final readout is qualitative, and in most cases not very sensitive, then these devices are for the most part limited as screening tests. Even though the incorporation of fluorophore labels and subsequently the optical components for the fluorescence readout to handheld devices increases the overall cost of the rapid diagnostic tests, the sensitivity of the rapid diagnostic tests is significantly improved and the quantitative assessment of the analyte present in a sample can be made.

Ultimately, rapid diagnostic tests should have the speed and the simplicity of lateral-flow assays and the quantitative

nature of ELISAs or fluorescence-based immunoassays. With this goal in sight, we have reviewed the combined use of microwave heating and plasmonic nanostructures for their potential applicability to rapid clinical diagnostics.[59] In this regard, we have reviewed several new approaches to rapid clinical diagnostics ranging from solution-based aggregation assays, to fluorescence- and chemiluminescence-based protein and DNA hybridization assays on planar sample geometries. In these approaches, microwave heating is used to selectively heat the water (in bulk solution) over the plasmonic nanostructures, to create a temperature gradient between the bulk solution and the nanostructures themselves. Target biomolecules present in the warmer bulk solution migrate towards the colder plasmonic nanostructures that support the biorecognition partners, where the biorecognition events occur, resulting in a measurable optical signal. We have shown that these techniques allow bioassays to be run in human serum and whole blood and can be completed in less than a minute, providing exciting new alternatives to current rapid clinical and bioagent diagnostic tests.

Acknowledgements

The authors acknowledge the Middle Atlantic Regional Center of Excellence for Biodefense and Emerging Infectious Diseases Research (NIH NIAID – U54 AI057168), and the American Heart Association (Beginning-in-Aid Grant to K. A.). Salary support to authors from UMBI and the IoF is also acknowledged.

References

1 E. I. Laderman, E. Whitworth, E. Dumaual, M. Jones, A. Hudak, W. Hogrefe, J. Carney and J. Groen, *Clin. Vaccine Immunol.*, 2008, **15**, 159–163.
2 D. R. Bienek, R. E. Biagini, D. G. Charlton, J. P. Smith, D. L. Sammons and S. A. Robertson, *Clin. Vaccine Immunol.*, 2008, **15**, 644–649.
3 R. Pastoor, M. Hatta, T. H. Abdoel and H. L. Smits, *Diagnostic Microbiol. Infect. Dis.*, 2008, **61**, 129–134.
4 C. C. Moore, S. T. Jacob, R. Pinkerton, D. B. Meya, H. Mayanja-Kizza, S. J. Reynolds and W. M. Scheld, *Clin. Infect. Dis.*, 2008, **46**, 215–222.
5 S. Wittfooth, Q. P. Qin and K. Pettersson, *Clin. Chem. Lab. Med.*, 2008, **46**, 18–20.
6 A. Skurup, T. Kristensen and G. Wennecke, *Clin. Chem. Lab. Med.*, 2008, **46**, 3–8.
7 M. A. Dineva, L. MahiLum-Tapay and H. Lee, *Analyst*, 2007, **132**, 1193–1199.
8 S. E. Letant, J. I. Ortiz, L. F. Bentley Tammero, J. M. Birch, R. W. Derlet, S. Cohen, D. Manning and M. T. McBride, *J. Clin. Microbiol.*, 2007, **45**, 3498–3505.
9 C. C. Kang, C. C. Chang, T. C. Chang, L. J. Liao, P. J. Lou, W. Xie and E. S. Yeung, *Analyst*, 2007, **132**, 745–749.
10 K. Nielsen, W. L. Yu, L. Kelly, R. Bermudez, T. Renteria, A. Dajer, E. Gutierrez, J. Williams, J. Algire and S. T. de Eschaide, *J. Immunoassay Immunochem.*, 2008, **29**, 10–18.
11 L. Liu, C. Peng, Z. Jin and C. Xu, *Biomed. Chromatogr.*, 2007, **21**, 861–866.
12 F. Ketema, C. Zeh, D. C. Edelman, R. Saville and N. T. Constantine, *J. Acquired Immune Defic. Syndr.*, 2001, **27**, 63–70.
13 C. D. Chin, V. Linder and S. K. Sia, *Lab Chip*, 2007, **7**, 41–57.
14 K. A. Spencer, F. A. Osorio and J. A. Hiscox, *Vaccine*, 2007, **25**, 5653–5659.
15 A. Bange, H. B. Halsall and W. R. Heineman, *Biosens. Bioelectron.*, 2005, **20**, 2488–2503.
16 K. Aslan and C. D. Geddes, *Anal. Chem.*, 2007, **79**, 2131–2136.
17 K. Aslan and C. D. Geddes, *Anal. Chem.*, 2005, **77**, 8057–8067.
18 K. Aslan and C. D. Geddes, *J. Fluoresc.*, 2006, **16**, 3–8.
19 K. Aslan and C. D. Geddes, *Plasmonics*, 2006, **1**, 53–59.
20 K. Aslan, P. Holley and C. D. Geddes, *J. Immunol. Methods*, 2006, **312**, 137–147.
21 K. Aslan, S. N. Malyn, G. Bector and C. D. Geddes, *Analyst*, 2007, **132**, 1122–1129.
22 K. Aslan, S. N. Malyn and C. D. Geddes, *Biochem. Biophys. Res. Commun.*, 2006, **348**, 612–617.
23 K. Aslan, S. N. Malyn and C. D. Geddes, *J. Immunol. Methods*, 2007, **323**, 55–64.
24 K. Aslan, Y. Zhang, S. Hibbs, L. Baillie, M. J. Previte and C. D. Geddes, *Analyst*, 2007, **132**, 1130–1138.
25 K. Aslan, S. N. Malyn and C. D. Geddes, *J. Am. Chem. Soc.*, 2006, **128**, 13372–13373.
26 M. J. Previte, K. Aslan, S. Malyn and C. D. Geddes, *J. Fluoresc.*, 2006, **16**, 641–647.
27 M. J. Previte, K. Aslan, S. N. Malyn and C. D. Geddes, *Anal. Chem.*, 2006, **78**, 8020–8027.
28 M. J. Previte and C. D. Geddes, *J. Fluoresc.*, 2007, **17**, 279–287.
29 K. Aslan, C. C. Luhrs and V. H. Perez-Luna, *J. Phys. Chem. B*, 2004, **108**, 15631–15639.
30 R. Elghanian, J. J. Storhoff, R. C. Mucic, R. L. Letsinger and C. A. Mirkin, *Science*, 1997, **277**, 1078–1081.
31 H. Li and L. Rothberg, *Proc. Natl. Acad. Sci. U. S. A.*, 2004, **101**, 14036–14039.
32 H. Li and L. J. Rothberg, *Anal. Chem.*, 2004, **76**, 5414–5417.
33 C. P. Chan, Y. C. Cheung, R. Renneberg and M. Seydack, *Adv. Biochem. Eng. Biotechnol.*, 2008, **109**, 123–154.
34 K. Aslan, J. R. Lakowicz and C. D. Geddes, *Anal. Biochem.*, 2004, **330**, 145–155.
35 K. Aslan, J. R. Lakowicz and C. D. Geddes, *Anal. Chem.*, 2005, **77**, 2007–2014.
36 X. Xu, M. S. Han and C. A. Mirkin, *Angew. Chem., Int. Ed.*, 2007, **46**, 3468–3470.
37 J. Yguerabide and E. E. Yguerabide, *Anal. Biochem.*, 1998, **262**, 137–156.
38 J. Yguerabide and E. E. Yguerabide, *Anal. Biochem.*, 1998, **262**, 157–176.
39 K. Aslan, P. Holley, L. Davies, J. R. Lakowicz and C. D. Geddes, *J. Am. Chem. Soc.*, 2005, **127**, 12115–12121.
40 M. J. Kogan, N. G. Bastus, R. Amigo, D. Grillo-Bosch, E. Araya, A. Turiel, A. Labarta, E. Giralt and V. F. Puntes, *Nano Lett.*, 2006, **6**, 110–115.
41 E. T. Thostenson and T. W. Chou, *Composites Part A: Appl. Sci. Manuf.*, 1999, **30**, 1055–1071.
42 Y. Zhang, K. Aslan, M. J. R. Previte and C. D. Geddes, *Dyes Pigm.*, 2008, **77**, 545–549.
43 K. Aslan, R. Badugu, J. R. Lakowicz and C. D. Geddes, *J. Fluoresc.*, 2005, **15**, 99–104.
44 M. J. Previte, Y. Zhang, K. Aslan and C. D. Geddes, *J. Fluoresc.*, 2007, **17**, 639–642.
45 K. Aslan, I. Gryczynski, J. Malicka, E. Matveeva, J. R. Lakowicz and C. D. Geddes, *Curr. Opin. Biotechnol.*, 2005, **16**, 55–62.
46 K. Aslan, J. Huang, G. M. Wilson and C. D. Geddes, *J. Am. Chem. Soc.*, 2006, **128**, 4206–4207.
47 M. H. Chowdhury, K. Aslan, S. N. Malyn, J. R. Lakowicz and C. D. Geddes, *J. Fluoresc.*, 2006, **16**, 295–299.
48 M. H. Chowdhury, K. Aslan, S. N. Malyn, J. R. Lakowicz and C. D. Geddes, *Appl. Phys. Lett.*, 2006, **88**, 173104.
49 M. J. Previte, K. Aslan and C. D. Geddes, *Anal. Chem.*, 2007, **79**, 7042–7052.
50 T. Liebermann and W. Knoll, *Colloids Surf., A*, 2000, **171**, 115–130.
51 T. Liebermann, W. Knoll, P. Sluka and R. Herrmann, *Colloids Surf., A*, 2000, **169**, 337–350.
52 W. H. Weber and C. F. Eagen, *Opt. Lett.*, 1979, **4**, 236–238.
53 R. E. Benner, R. Dornhaus and R. K. Chang, *Opt. Commun.*, 1979, **30**, 145–149.
54 W. H. Weber and C. F. Eagen, *Bull. Am. Phys. Soc.*, 1979, **24**, 441–441.
55 W. Knoll, M. R. Philpott and J. D. Swalen, *J. Chem. Phys.*, 1981, **75**, 4795–4799.
56 D. Guenter, J. Greer, A. Barbara, G. Robinson, J. Roberts and G. Browne, *AIDS Patient Care STDs*, 2008, **22**, 195–204.
57 K. Aslan, M. J. Previte, Y. Zhang and C. D. Geddes, *J. Immunol. Methods*, 2008, **331**, 103–113.
58 E. G. Matveeva, Z. Gryczynski, J. Malicka, J. Lukomska, S. Makowiec, K. W. Berndt, J. R. Lakowicz and I. Gryczynski, *Anal. Biochem.*, 2005, **344**, 161–167.
59 K. Aslan and C. D. Geddes, *Plasmonics*, 2008, **2–3**, 89–101.

